Supporting Information

Immobilization of N-oxide functionality into NbO-type MOFs for significantly enhanced C_2H_2/CH_4 and CO_2/CH_4 separations

Tingting Xu, Lihui Fan, Zhenzhen Jiang, Ping Zhou, Ziruo Li, Huangyan Lu and Yabing He*

Key Laboratory of the Ministry of Education for Advanced Catalysis Materials, College of Chemistry and Life Sciences, Zhejiang Normal University, Jinhua 321004, China. E-mail: heyabing@zjnu.cn

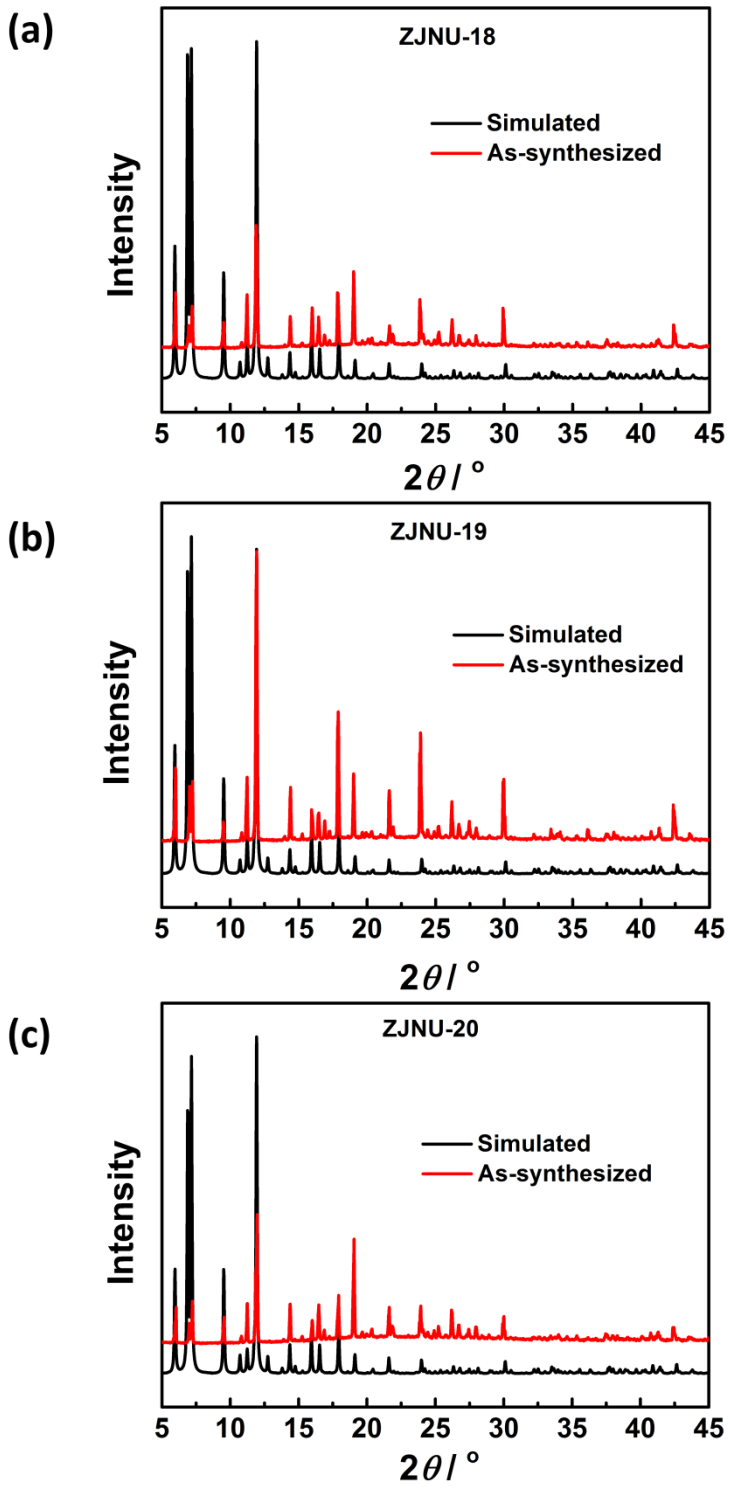

Fig. S1 The experimental and simulated PXRD patterns of (a) **ZJNU-18**, (b) **ZJNU-19**, and (c) **ZJNU-20**.

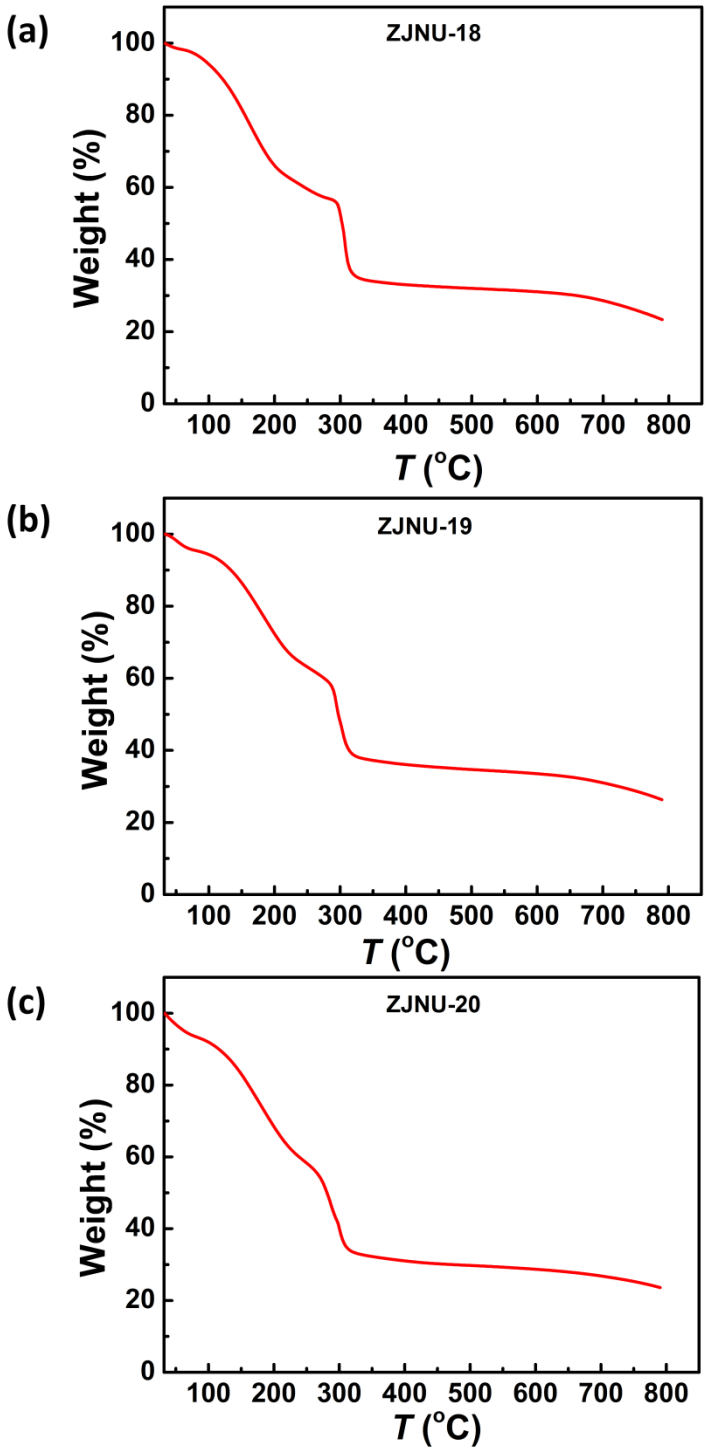

Fig. S2 TGA curves of the as-synthesized (a) **ZJNU-18**, (b) **ZJNU-19**, and (c) **ZJNU-20** under N_2 atmosphere.

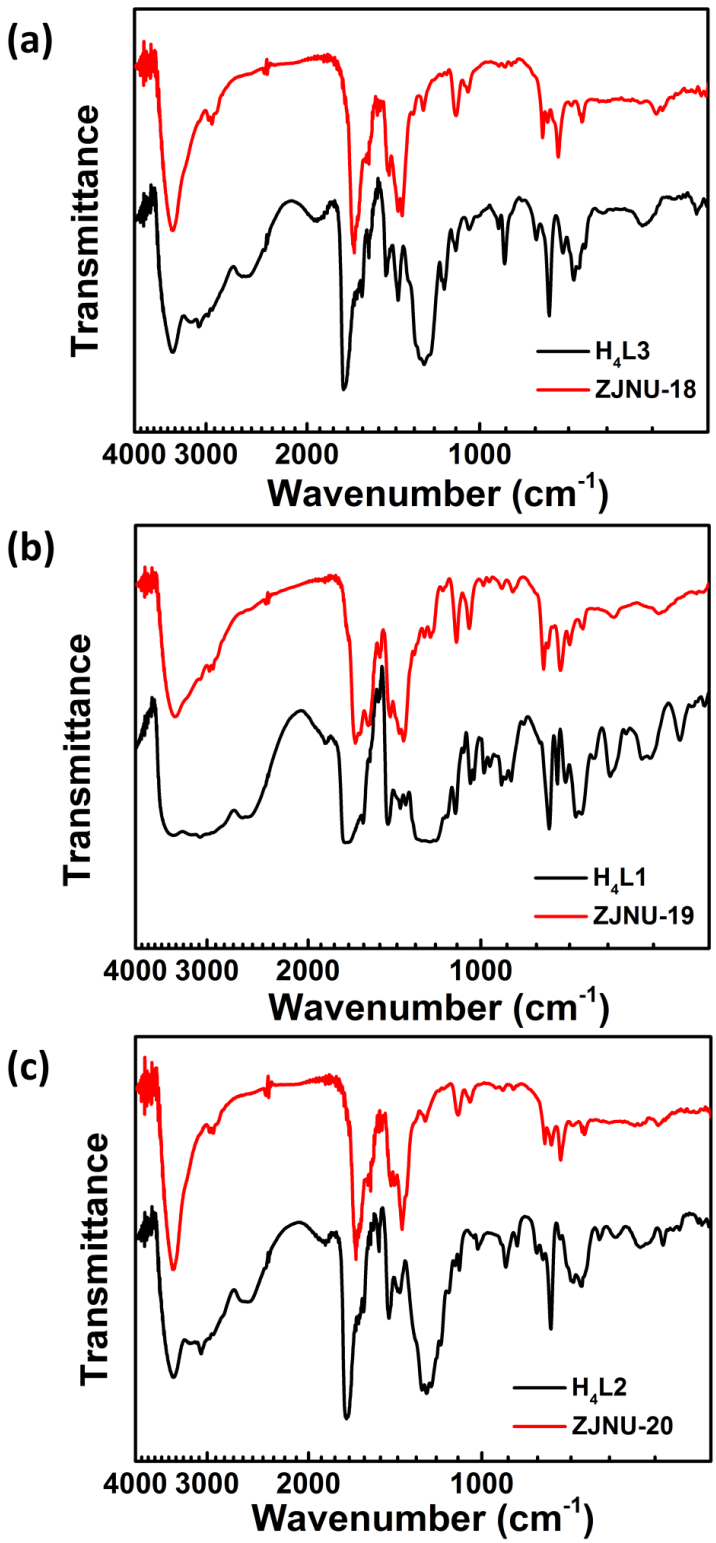

Fig. S3 Comparison of FTIR spectra of (a) **ZJNU-18** and its ligand H_4L3, (b) **ZJNU-19** and its ligand H_4L1, and (c) **ZJNU-20** and its ligand H_4L2.

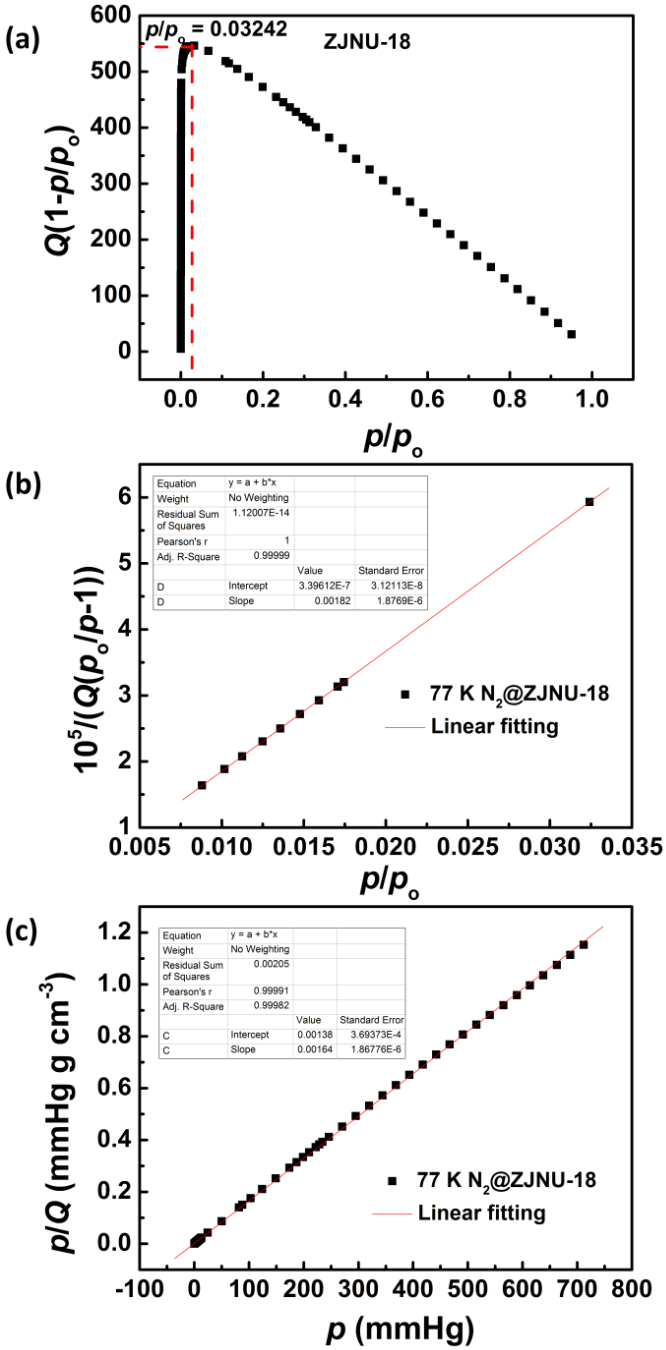

S_{BET} = 1/(3.39612×10^{-7}+ 0.00182)/22414 ×6.023 ×10^{23} ×0.162 ×10^{-18} = 2391 m^2 g^{-1}

$S_{Langmuir}$ = (1/0.00164)/22414 ×6.023 ×10^{23} ×0.162 ×10^{-18} = 2654 m^2 g^{-1}

BET constant C = 1 + 0.00182/3.39612×10^{-7} = 5360

$$(p/p_o)_{n_m} = \frac{1}{\sqrt{C}+1} = 0.01347$$

Fig. S4 The consistency plot (a), BET surface area plot (b), and Langmuir surface area plot (c) for **ZJNU-18**.

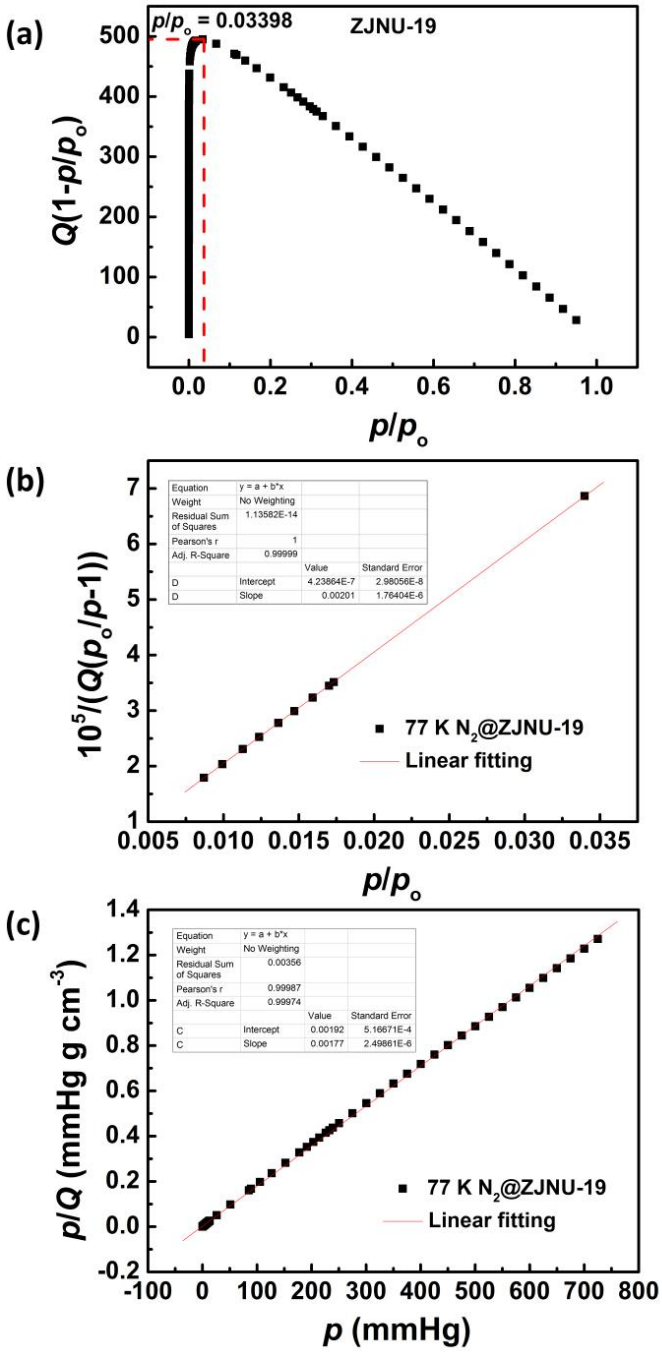

S_{BET} = 1/(4.23864×10^{-7}+ 0.00201)/22414 × 6.023 × 10^{23} × 0.162 × 10^{-18} = 2165 m^2 g^{-1}

$S_{Langmuir}$ = (1/0.00177)/22414 × 6.023 × 10^{23} × 0.162 × 10^{-18} = 2459 m^2 g^{-1}

BET constant C = 1 + 0.00201/4.23864×10^{-7} = 4743

$$(p/p_o)_{n_m} = \frac{1}{\sqrt{C}+1} = 0.01431$$

Fig. S5 The consistency plot (a), BET surface area plot (b), and Langmuir surface area plot (c) for **ZJNU-19**.

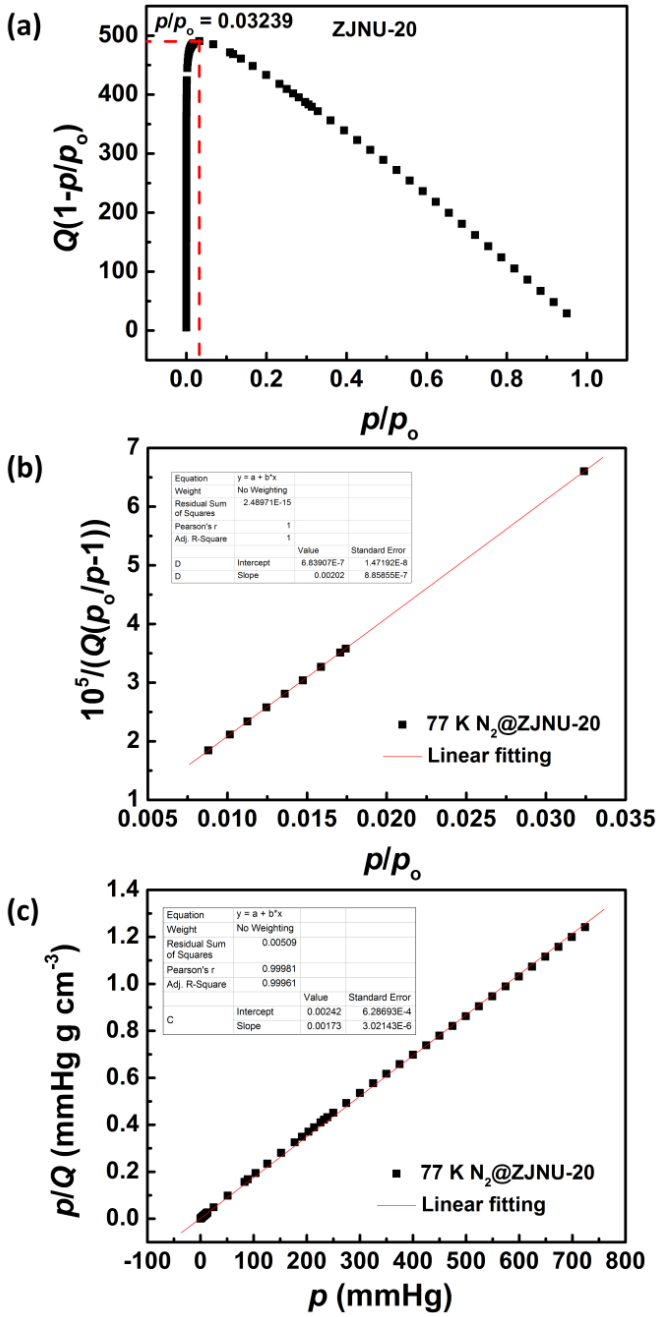

S_{BET} = 1/(6.83907×10^{-7}+ 0.00202)/22414 ×6.023 ×10^{23} ×0.162 ×10^{-18} = 2154 m^2 g^{-1}

$S_{Langmuir}$ = (1/0.00173)/22414 ×6.023 ×10^{23} ×0.162 ×10^{-18} = 2516 m^2 g^{-1}

BET constant C = 1 + 0.00202/6.83907×10^{-7} = 2955

$$(p/p_o)_{n_m} = \frac{1}{\sqrt{C}+1} = 0.01806$$

Fig. S6 The consistency plot (a), BET surface area plot (b), and Langmuir surface area plot (c) for **ZJNU-20**.

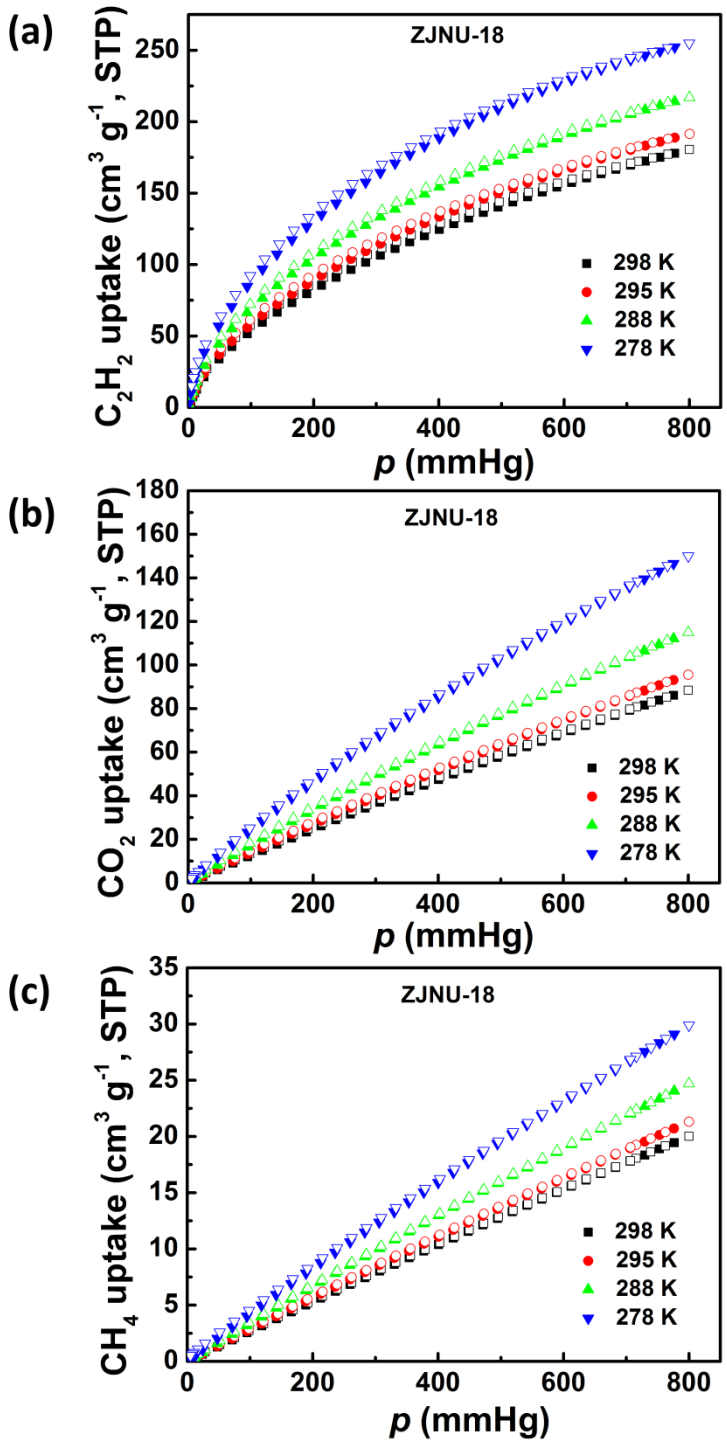

Fig. S7 Pure-component isotherms of (a) C_2H_2, (b) CO_2, and (c) CH_4 in **ZJNU-18** at four different temperatures of 298 K, 295 K, 288 K, and 278 K. Solid and open symbols represent adsorption and desorption data, respectively. STP stands for standard temperature and pressure.

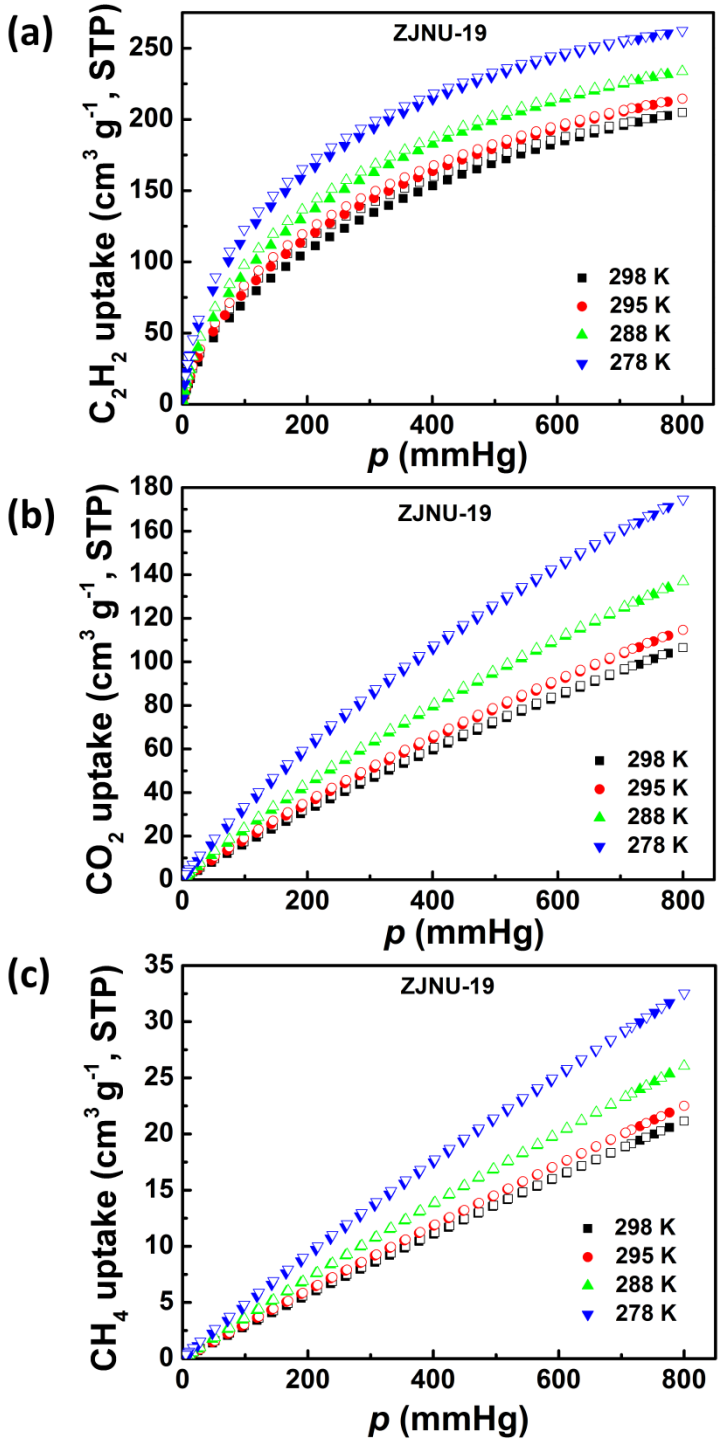

Fig. S8 Pure-component isotherms of (a) C_2H_2, (b) CO_2, and (c) CH_4 in **ZJNU-19** at four different temperatures of 298 K, 295 K, 288 K, and 278 K. Solid and open symbols represent adsorption and desorption data, respectively. STP stands for standard temperature and pressure.

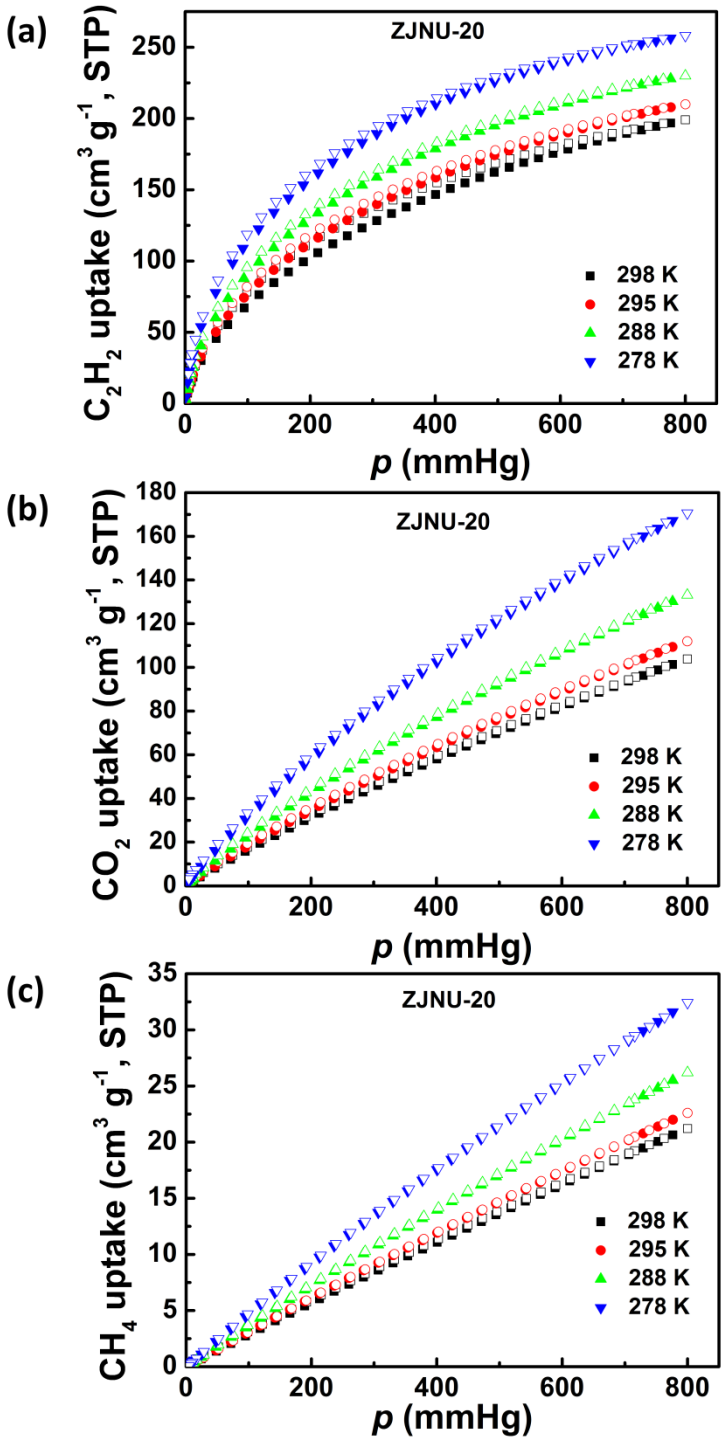

Fig. S9 Pure-component isotherms of (a) C_2H_2, (b) CO_2, and (c) CH_4 in **ZJNU-20** at four different temperatures of 298 K, 295 K, 288 K, and 278 K. Solid and open symbols represent adsorption and desorption data, respectively. STP stands for standard temperature and pressure.

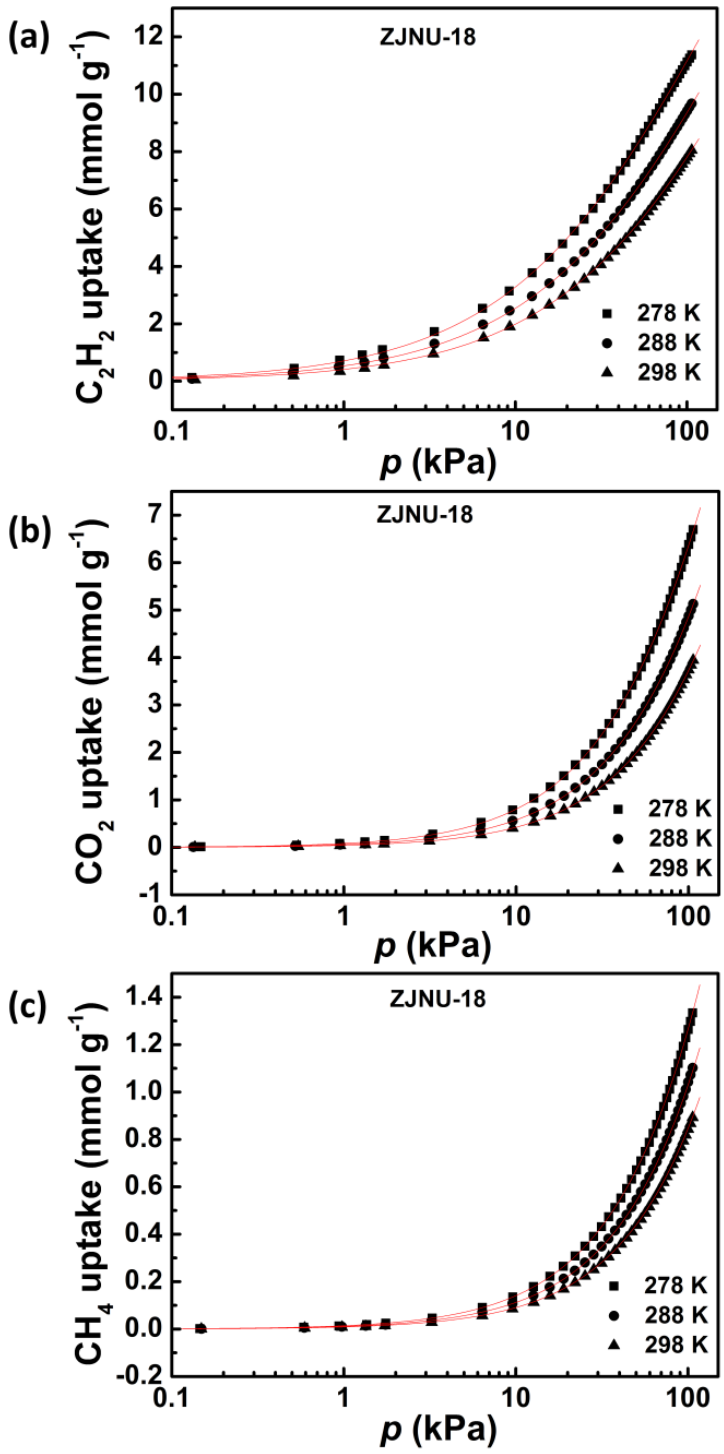

Fig. S10 Comparison of the pure-component isotherm data for (a) C_2H_2, (b) CO_2, and (c) CH_4 in **ZJNU-18** with the fitted isotherms at 278 K, 288 K, and 298 K.

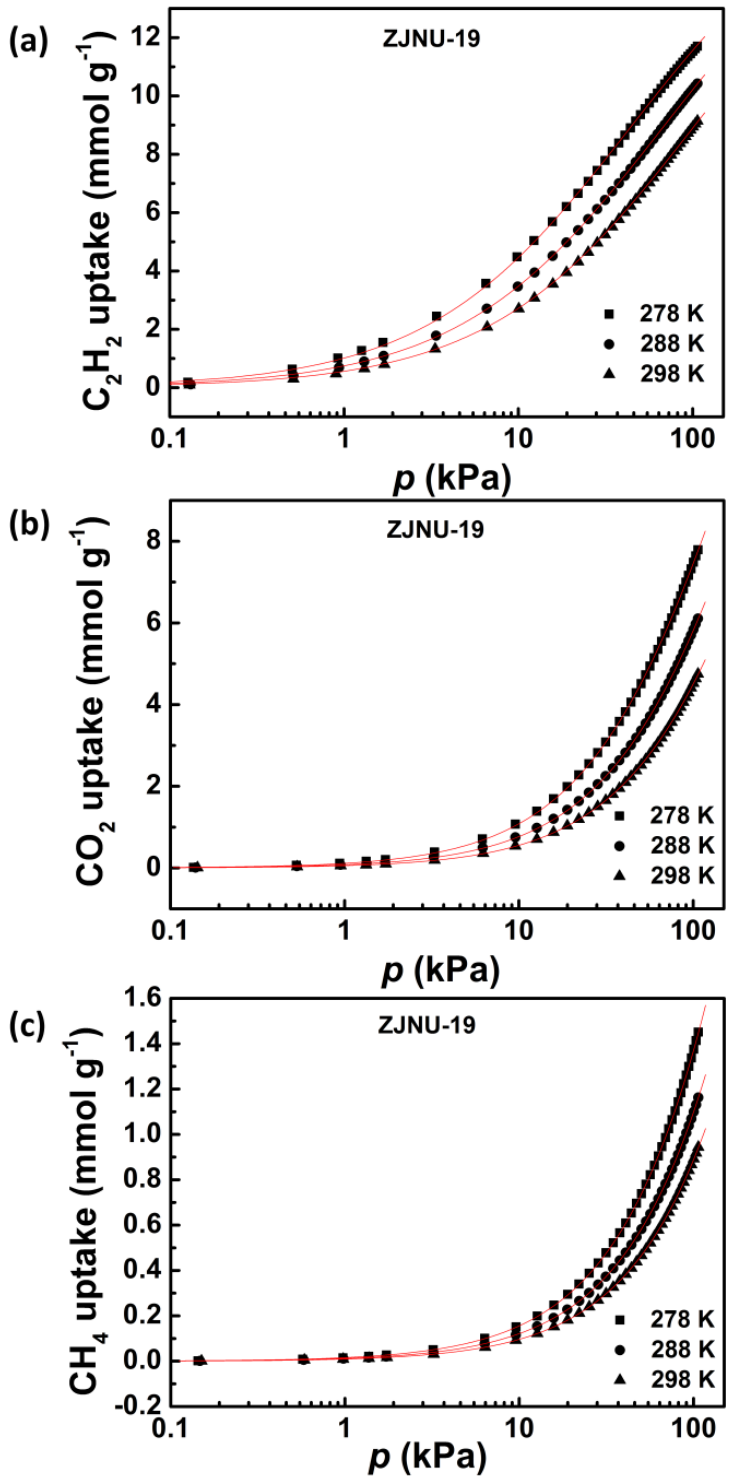

Fig. S11 Comparison of the pure-component isotherm data for (a) C_2H_2, (b) CO_2, and (c) CH_4 in **ZJNU-19** with the fitted isotherms at 278 K, 288 K, and 298 K.

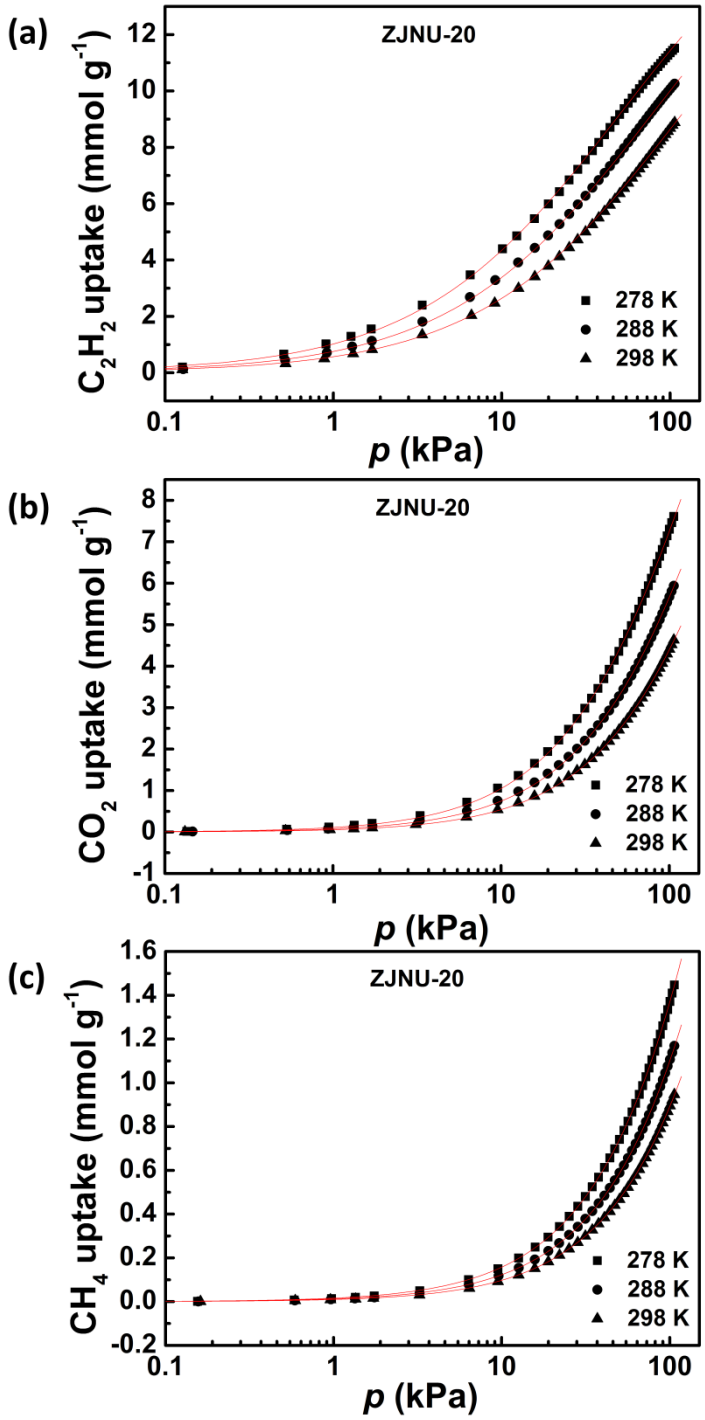

Fig. S12 Comparison of the pure-component isotherm data for (a) C_2H_2, (b) CO_2, and (c) CH_4 in **ZJNU-20** with the fitted isotherms at 278 K, 288 K, and 298 K.

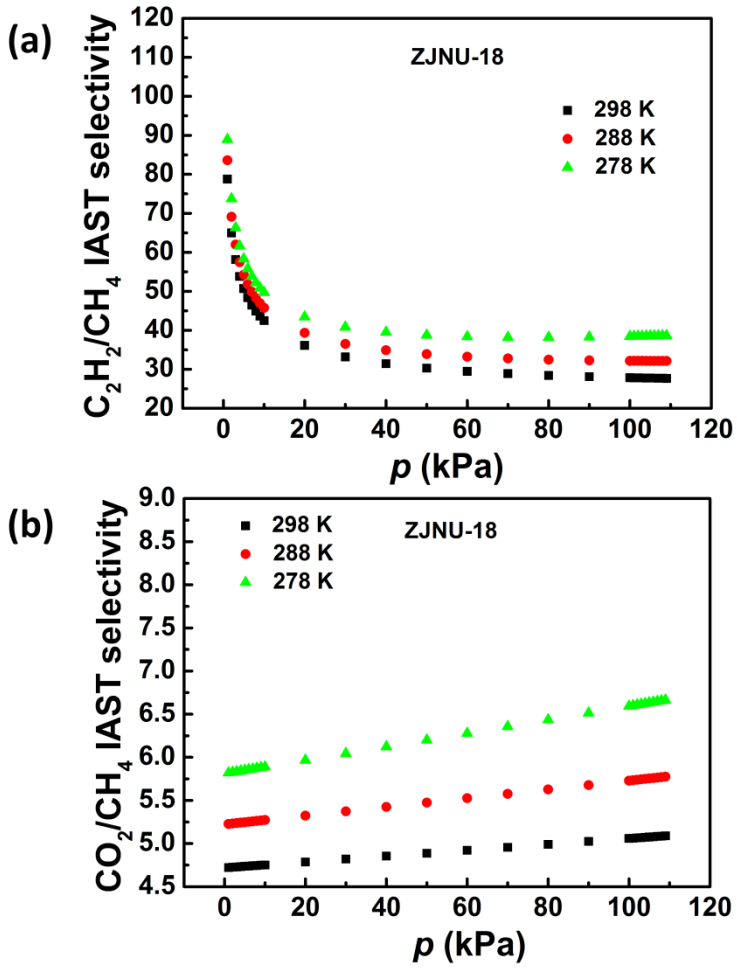

Fig. S13 IAST calculations of (a) C_2H_2/CH_4 and (b) CO_2/CH_4 adsorption selectivities of **ZJNU-18** for the equimolar binary gas mixtures at three different temperatures of 298 K, 288 K, and 278 K.

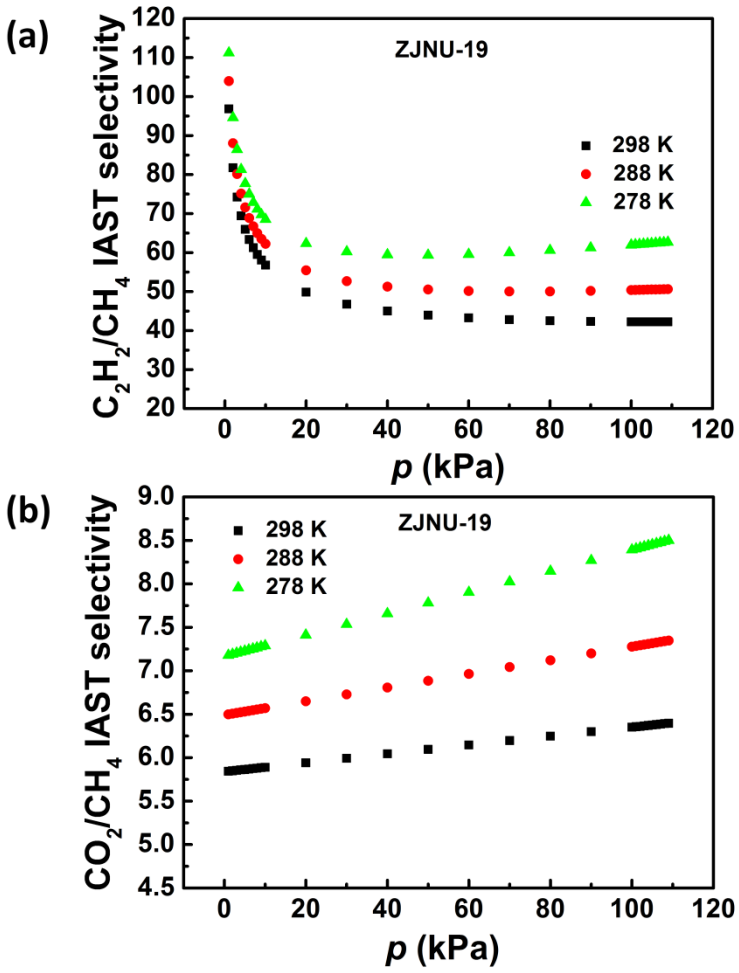

Fig. S14 IAST calculations of (a) C_2H_2/CH_4 and (b) CO_2/CH_4 adsorption selectivities of **ZJNU-19** for the equimolar binary gas mixtures at three different temperatures of 298 K, 288 K, and 278 K.

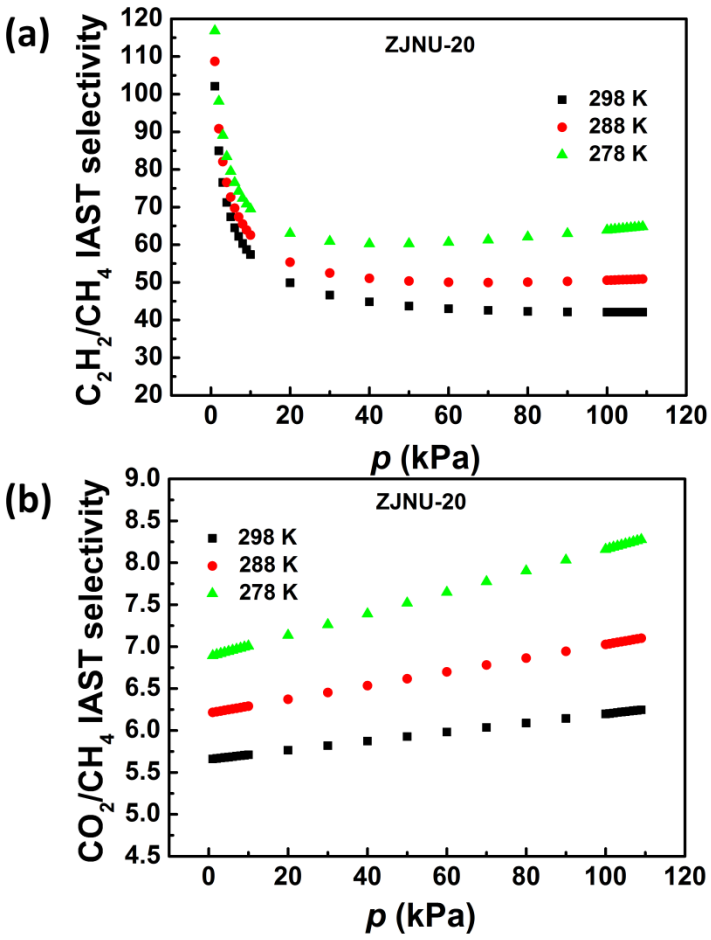

Fig. S15 IAST calculations of (a) C_2H_2/CH_4 and (b) CO_2/CH_4 adsorption selectivities of **ZJNU-20** for the equimolar binary gas mixtures at three different temperatures of 298 K, 288 K, and 278 K.

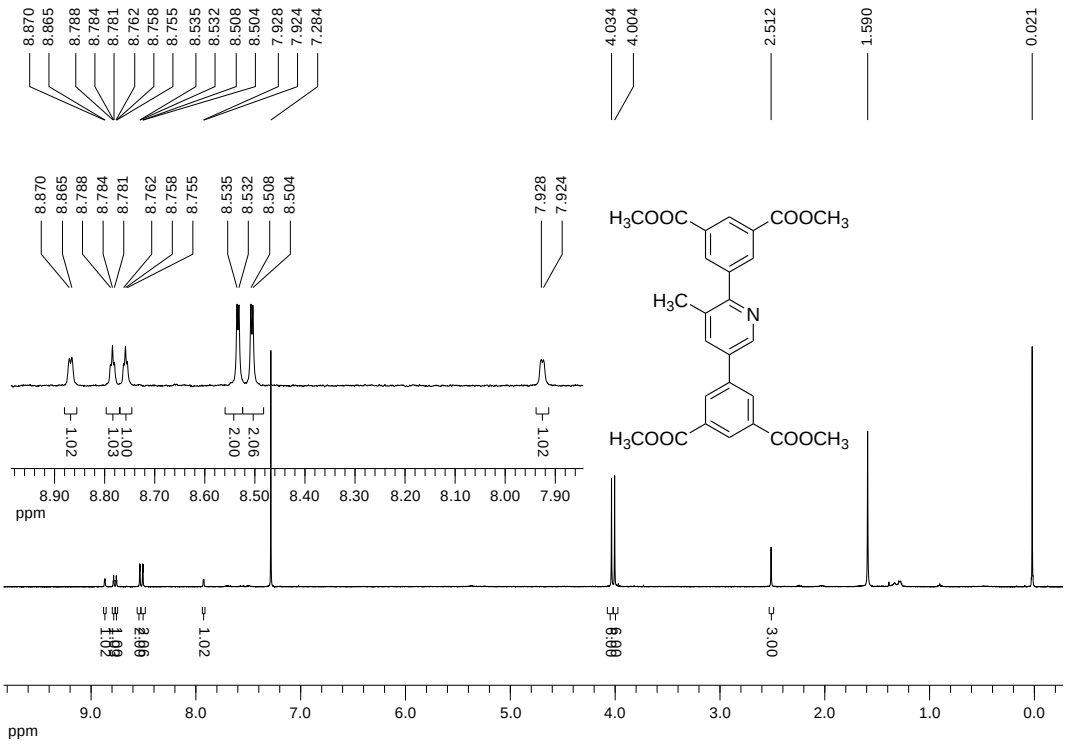
8.870
8.865
8.788
8.784
8.781
8.762
8.758
8.755
8.535
8.532
8.508
8.504
7.928
7.924
7.284
4.034
4.004
2.512
1.590
0.021
H3COOC
COOCH3
H3C
N
1.02
1.00
1.03
2.00
2.06
1.02
3.00
ppm

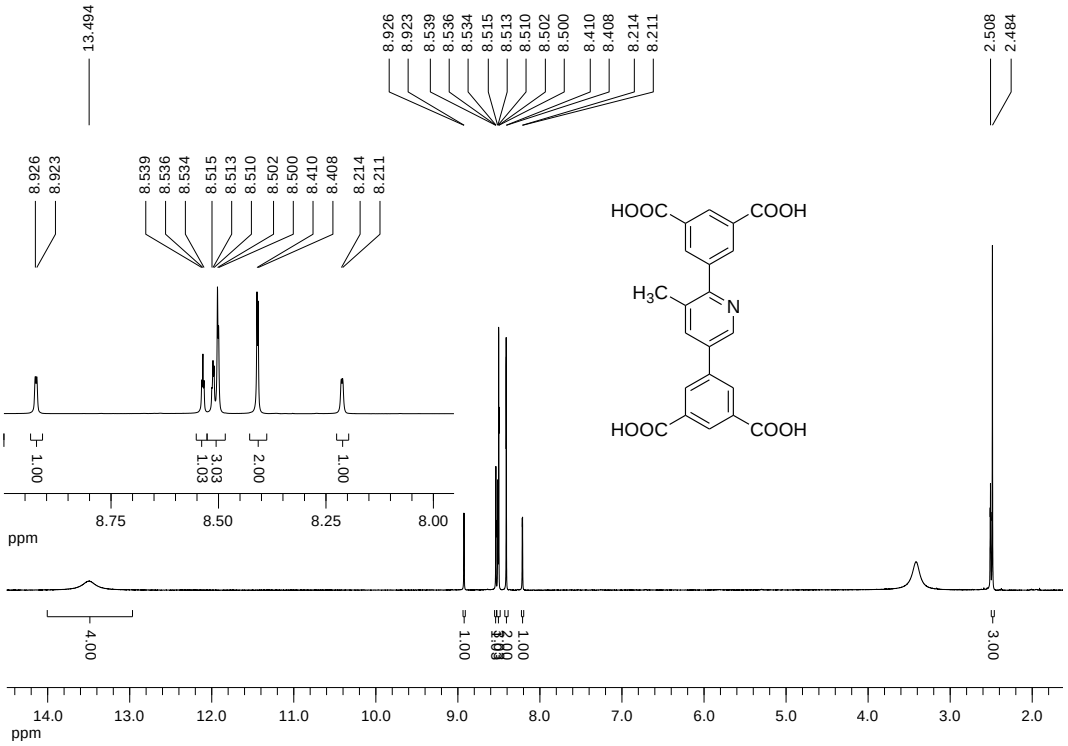
13.494
8.926
8.923
8.539
8.536
8.534
8.515
8.513
8.510
8.502
8.500
8.410
8.408
8.214
8.211
2.508
2.484
HOOC
COOH
H3C
N
1.00
3.03
2.00
1.00
4.00
1.00
3.00
ppm

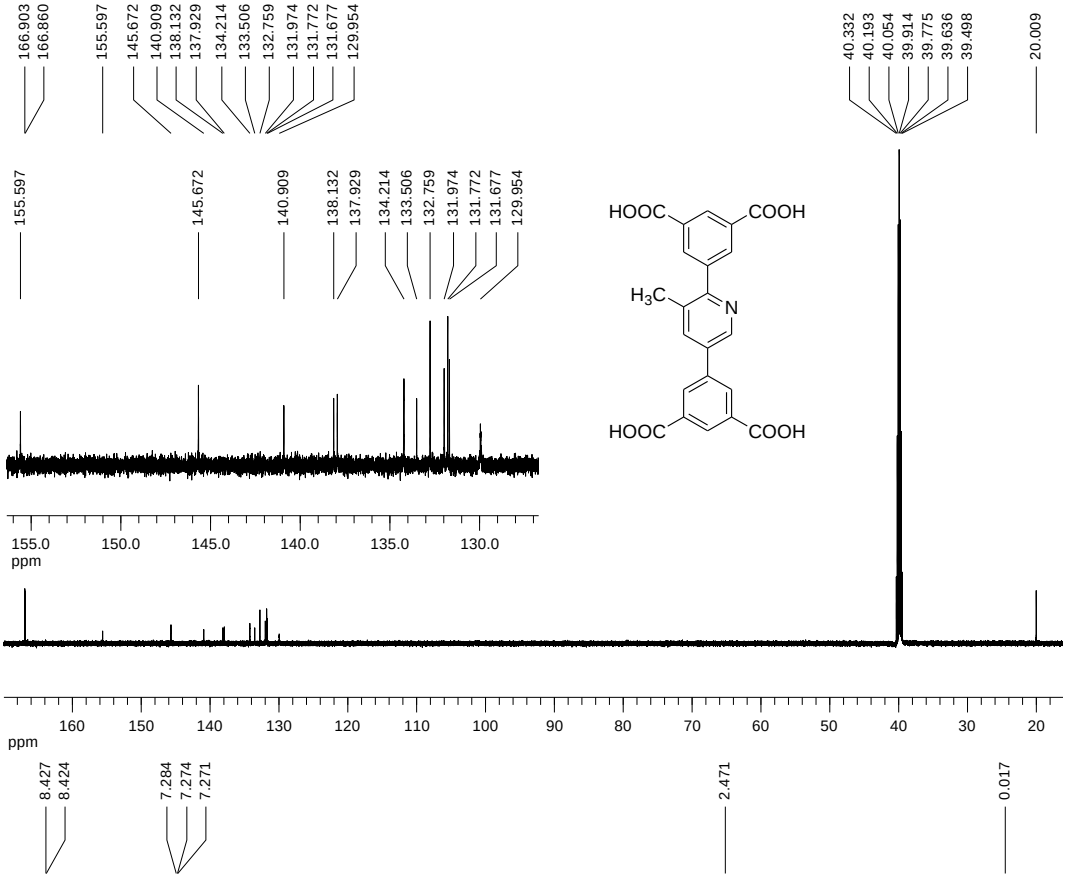
166.903
166.860
155.597
145.672
140.909
138.132
137.929
134.214
133.506
132.759
131.974
131.772
131.677
129.954
40.332
40.193
40.054
39.914
39.775
39.636
39.498
20.009
HOOC
COOH
H3C
N
HOOC
COOH
155.0
150.0
145.0
140.0
135.0
130.0
ppm
160
150
140
130
120
110
100
90
80
70
60
50
40
30
20
ppm

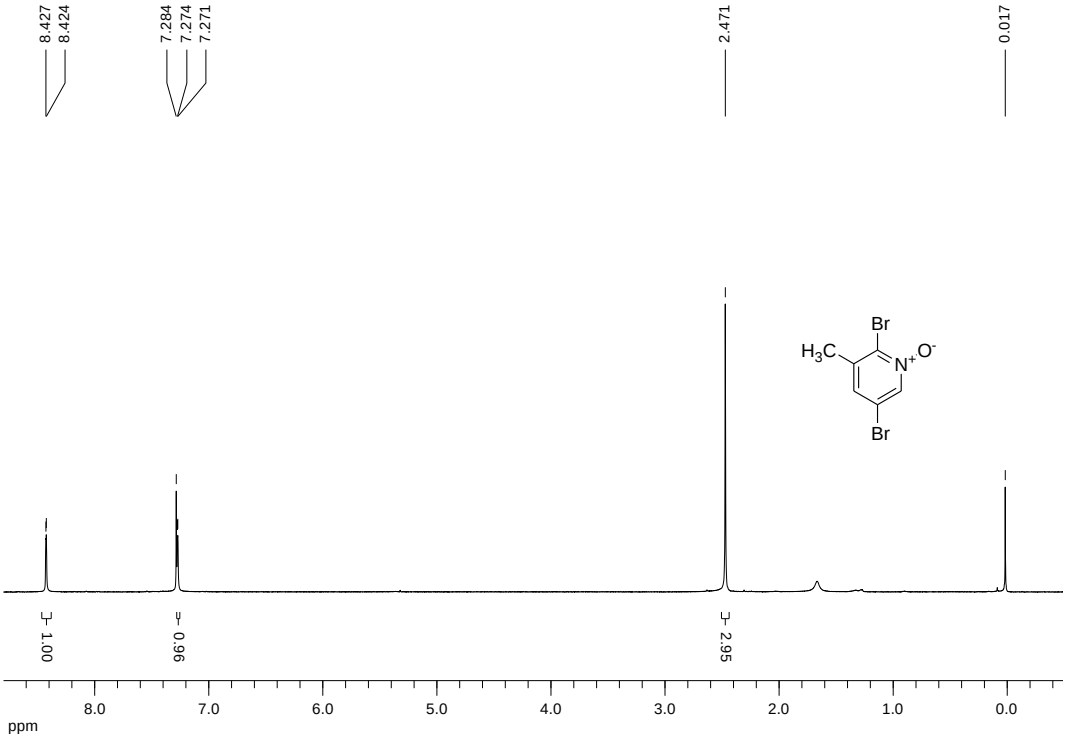
8.427
8.424
7.284
7.274
7.271
2.471
0.017
Br
H3C
N+
O-
Br
1.00
0.96
2.95
8.0
7.0
6.0
5.0
4.0
3.0
2.0
1.0
0.0
ppm

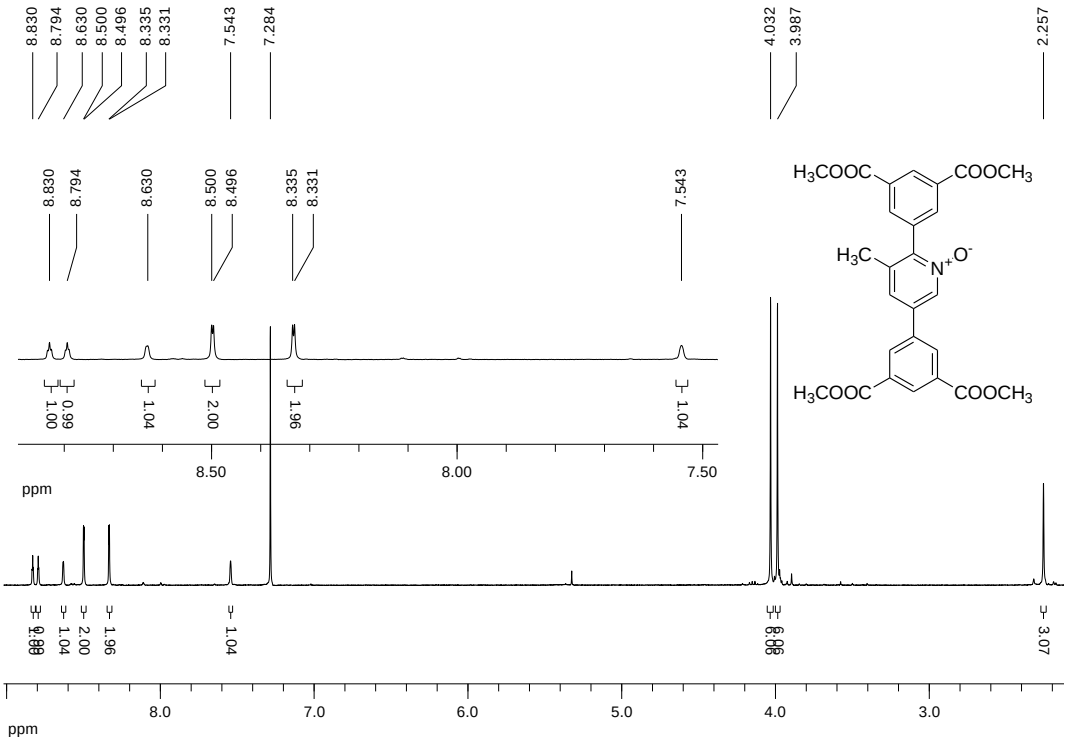
8.830
8.794
8.630
8.500
8.496
8.335
8.331
7.543
7.284
4.032
3.987
2.257
H3COOC
COOCH3
H3C
N+O-
1.00
0.99
1.04
2.00
1.96
1.04
6.06
3.07
8.50
8.00
7.50
ppm
8.0
7.0
6.0
5.0
4.0
3.0

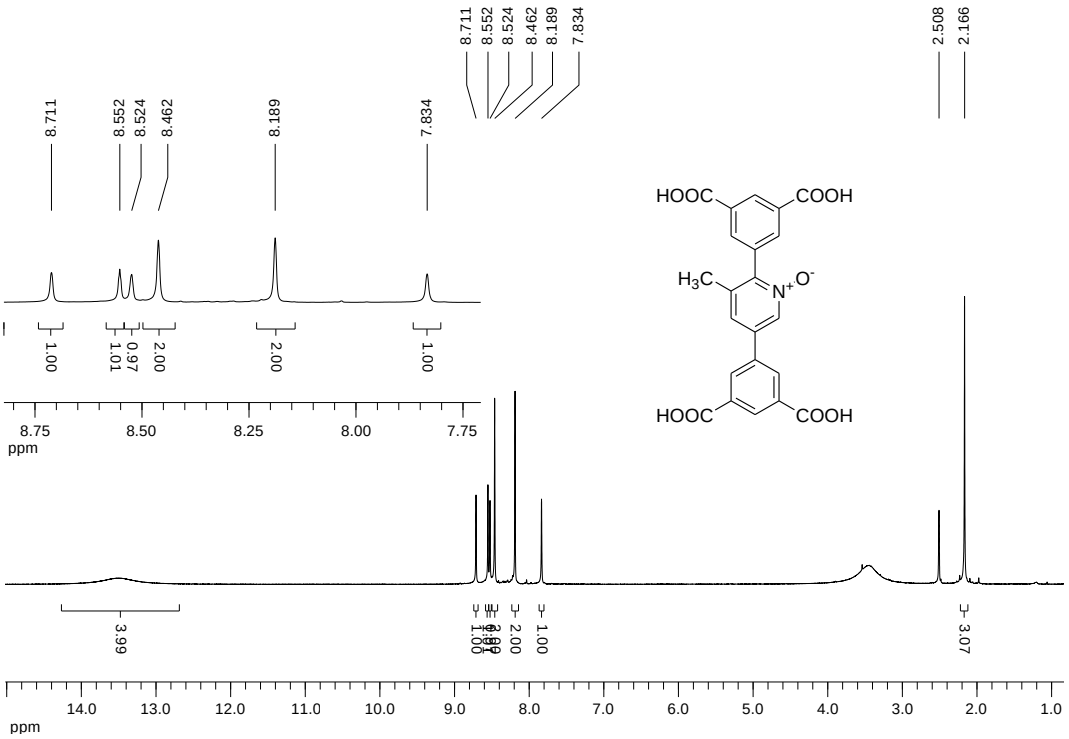
8.711
8.552
8.524
8.462
8.189
7.834
2.508
2.166
HOOC
COOH
H3C
N+O-
1.00
1.01
0.97
2.00
2.00
1.00
3.99
1.00
2.00
1.00
3.07
8.75
8.50
8.25
8.00
7.75
ppm
14.0
13.0
12.0
11.0
10.0
9.0
8.0
7.0
6.0
5.0
4.0
3.0
2.0
1.0

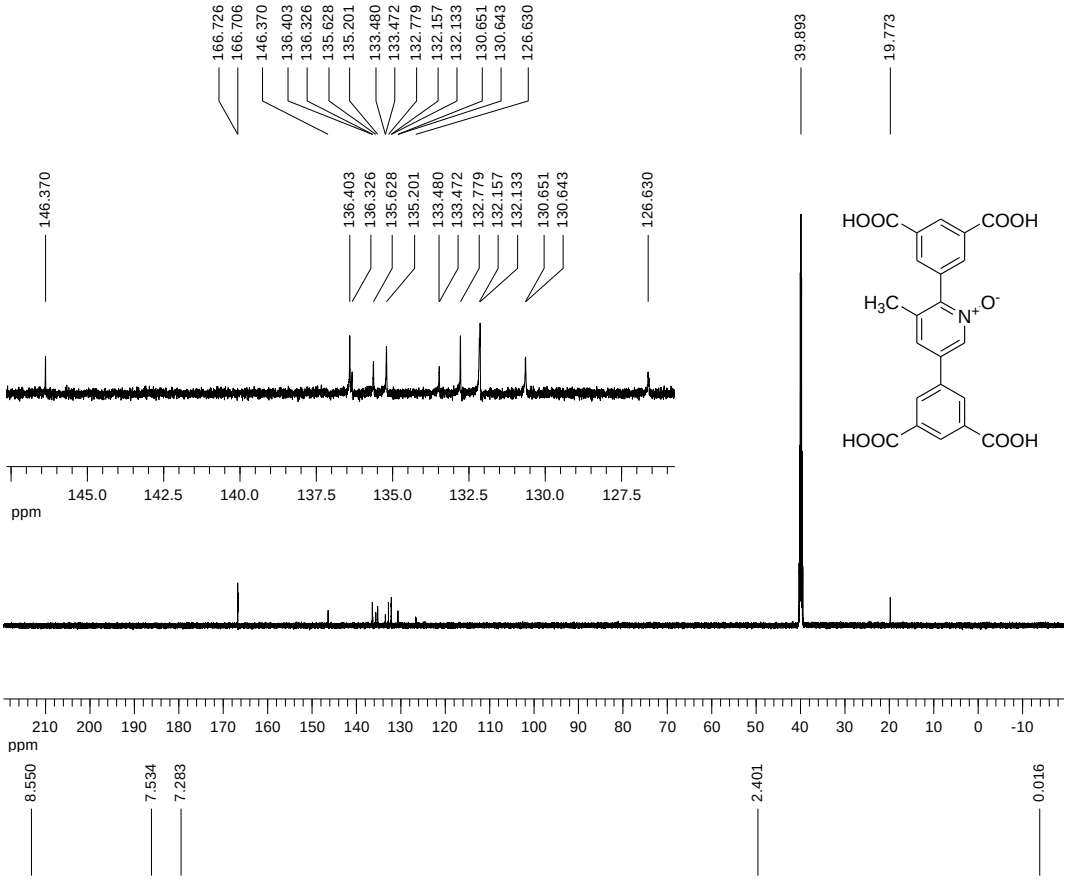
166.726
166.706
146.370
136.403
136.326
135.628
135.201
133.480
133.472
132.779
132.157
132.133
130.651
130.643
126.630
39.893
19.773
HOOC
COOH
H3C
N+
O-
HOOC
COOH
ppm
8.550
7.534
7.283
2.401
0.016

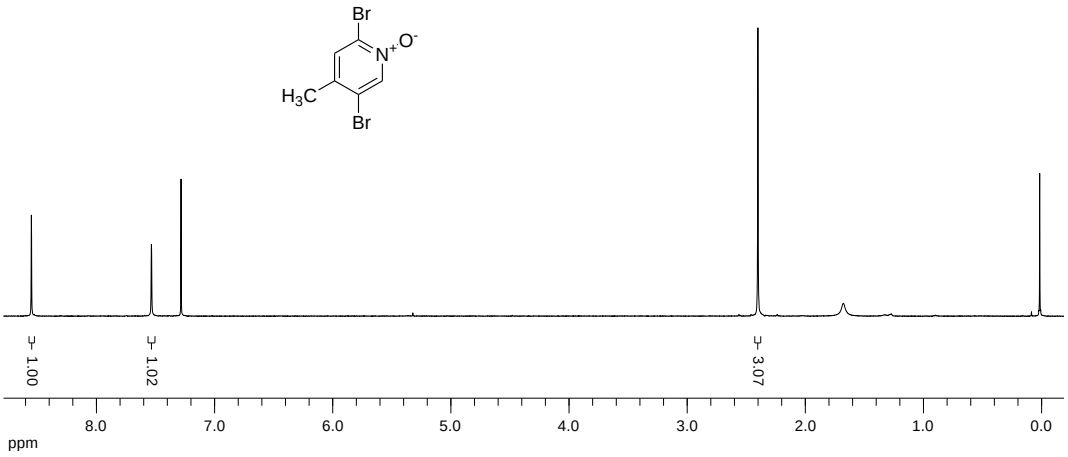
Br
N+
O-
H3C
Br
1.00
1.02
3.07
ppm

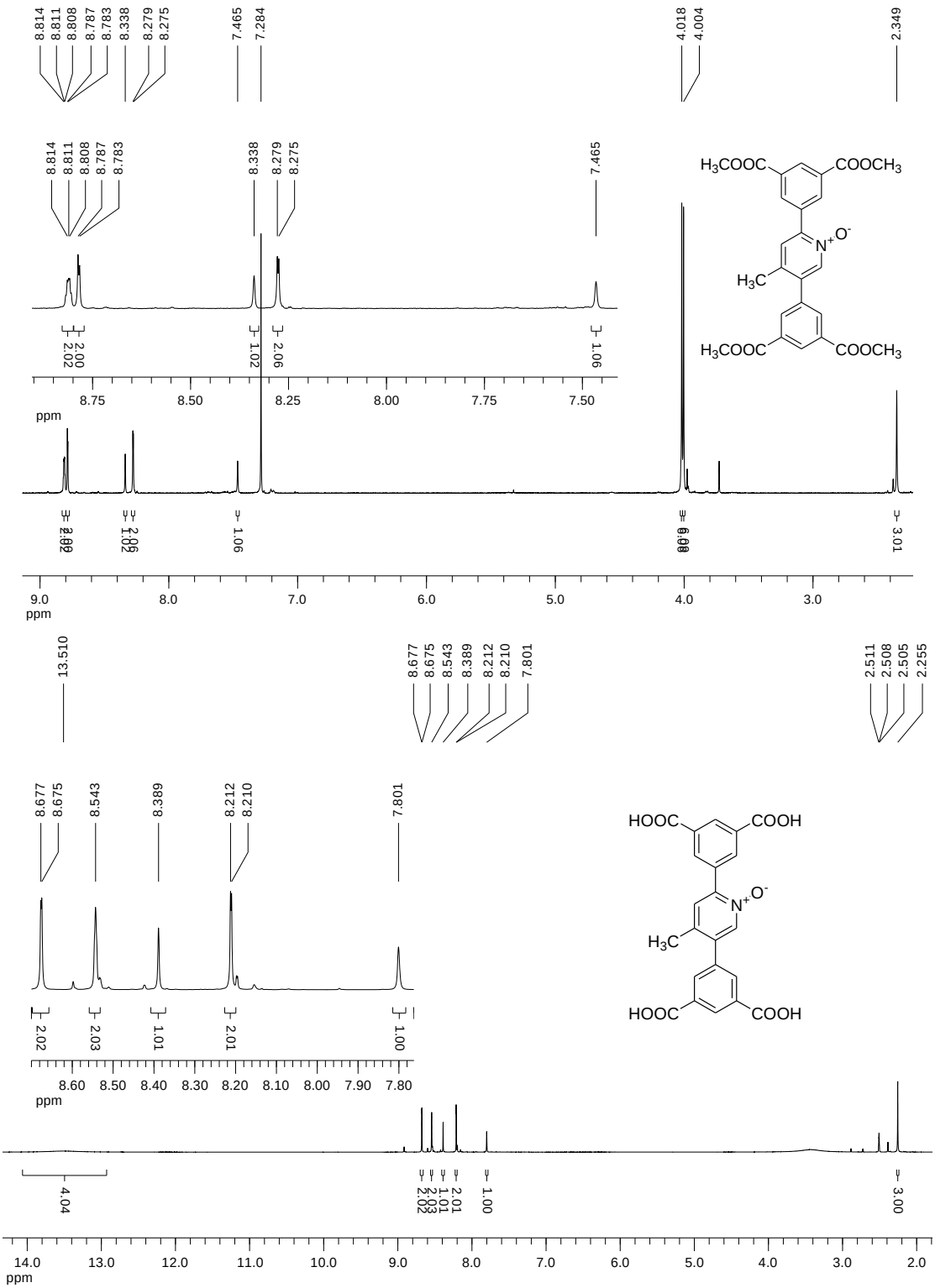
8.814
8.811
8.808
8.787
8.783
8.338
8.279
8.275
7.465
7.284
4.018
4.004
2.349
H3COOC
COOCH3
N+O-
H3C
ppm
13.510
8.677
8.675
8.543
8.389
8.212
8.210
7.801
2.511
2.508
2.505
2.255
HOOC
COOH
4.04
2.03
1.00
3.00

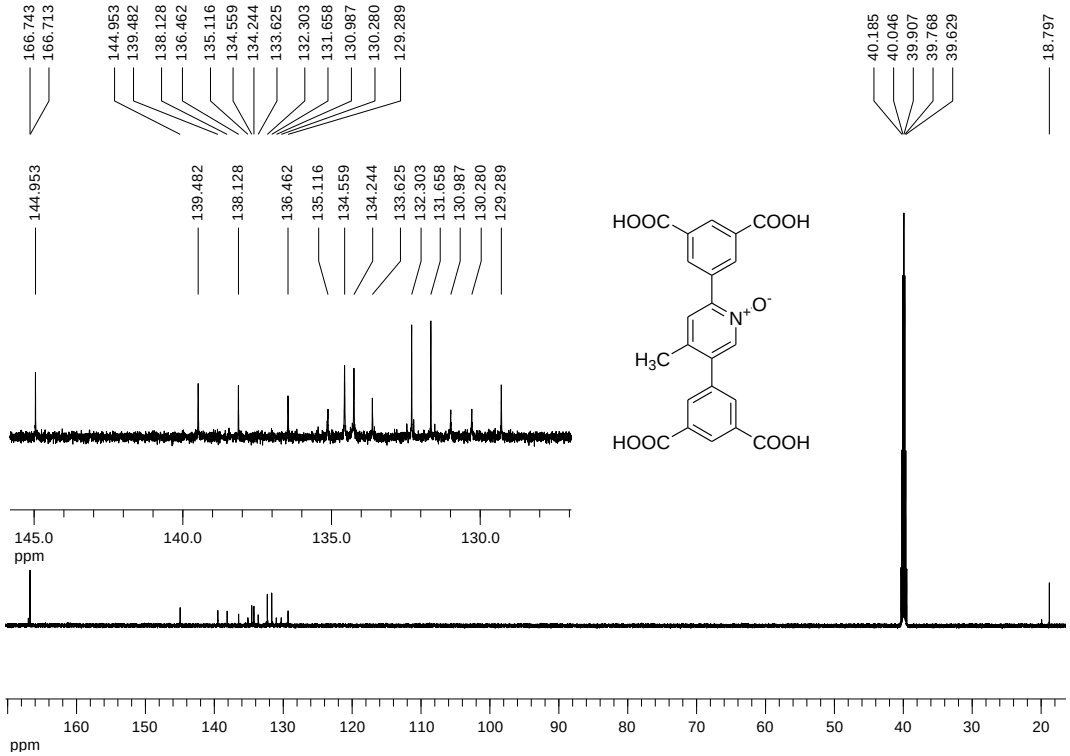

Fig. S16 ^{1}H and ^{13}C NMR spectra.

Table S1. Summarizes of physical parameters of C_2H_2, CO_2, and CH_4

Adsorbates	BP (K)	T_c (K)	p_c (bar)	Kinetic diameter (Å)	Molecular dimension (Å)	Polarizability ($\times10^{25}$ cm^3)	Dipole moment ($\times10^{18}$ esu cm)	Quadruple moment ($\times10^{26}$ esu cm^2)
C_2H_2	188.40	308.30	61.14	3.3	3.3×3.3×5.7	33.3-39.3	0	+7.5
CO_2	194.65	304.12	73.74	3.3	3.2×3.3×5.4	29.11	0	-4.3
CH_4	111.66	190.56	45.99	3.758	3.7×3.7×3.7	25.93	0	0

BP: normal boiling point; T_c: critical temperature; p_c: critical pressure

Table S2 Crystal data and structure refinement for **ZJNU-18**, **ZJNU-19**, and **ZJNU-20**.

MOFs	**ZJNU-18**	**ZJNU-19**	**ZJNU-20**
Empirical formula	$C_{37}H_{52}Cu_2N_6O_{16}$	$C_{37}H_{50}Cu_2N_6O_{16}$	$C_{37}H_{50}Cu_2N_6O_{16}$
Formula weight	963.92	961.91	961.91
λ (Å)	1.54178	0.71073	1.54178
Crystal system	Trigonal	Trigonal	Trigonal
Space group	*R-3m:H*	*R-3m:H*	*R-3m:H*
Unit cell dimensions	a = 18.5593(10) Å b = 18.5593(10) Å c = 38.480(2) Å α = 90° β = 90° γ = 120°	a = 18.6199(3) Å b = 18.6199(3) Å c = 38.2895(8) Å α = 90° β = 90° γ = 120°	a = 18.5543(7)) Å b = 18.5543(7) Å c = 38.4604(19) Å α = 90° β = 90° γ = 120°
V (Å^3)	11478.5(14)	11496.5(4)	11466.6(10)
Z	9	9	9
D_c (g cm^{-3})	1.255	1.250	1.254
μ (mm^{-1})	1.584	0.897	1.586
F(000)	4518	4500	4500
θ range for data collection (°)	4.765 to 72.206	2.708 to 27.494	2.980 to 72.417
Limiting indices	$-17 \le h \le 22$ $-22 \le k \le 22$ $-47 \le l \le 26$	$-24 \le h \le 23$ $-19 \le k \le 24$ $-37 \le l \le 49$	$-22 \le h \le 13$ $-22 \le k \le 17$ $-47 \le l \le 31$
Reflections collected / unique	16630 / 2733	19677 / 3157	12356 / 2761
R_{int}	0.0337	0.0183	0.0576
Refinement method	Full-matrix least-squares on F^2	Full-matrix least-squares on F^2	Full-matrix least-squares on F^2
Data/restraints/parameters	2733 / 92 / 122	3157 / 97 / 126	2761 / 99 / 131
Goodness-of-fit on F^2	1.083	1.078	0.970
Final R indices [$I > 2\sigma(I)$]	R_1 = 0.0430 wR_2 = 0.1334	R_1 = 0.0366 wR_2 = 0.1208	R_1 = 0.0515 wR_2 = 0.1443
R indices (all data)	R_1 = 0.0461 wR_2 = 0.1391	R_1 = 0.0386 wR_2 = 0.1227	R_1 = 0.0601 wR_2 = 0.1523
Largest diff. peak and hole (e·Å^{-3})	0.685 and -0.319	0.736 and -0.472	0.761 and -0.331
CCDC	1992051	1992049	1992050

Table S3 Langmuir-Freundlich parameters for adsorption of C_2H_2, CO_2, and CH_4 in **ZJNU-18**.

Adsorbates	q_{sat} (mmol g^{-1})	b_0 $(kPa)^{-v}$	E (kJ mol^{-1})	v	R^2
C_2H_2	26.45879	6.96469×10^{-6}	19.139	0.71195	0.99986
CO_2	27.00081	1.79578×10^{-7}	22.531	1	0.99998
CH_4	10.88758	1.7423×10^{-6}	15.310	1	0.99987

Table S4 Langmuir-Freundlich parameters for adsorption of C_2H_2, CO_2, and CH_4 in **ZJNU-19**.

Adsorbates	q_{sat} (mmol g^{-1})	b_0 $(kPa)^{-v}$	E (kJ mol^{-1})	v	R^2
C_2H_2	17.81701	6.16506×10^{-6}	21.237	0.74305	0.9999
CO_2	21.53152	1.70584×10^{-7}	23.905	1	0.99997
CH_4	10.06031	1.11068×10^{-6}	16.773	1	0.99999

Table S5 Langmuir-Freundlich parameters for adsorption of C_2H_2, CO_2, and CH_4 in **ZJNU-20**.

Adsorbates	q_{sat} (mmol g^{-1})	b_0 $(kPa)^{-v}$	E (kJ mol^{-1})	v	R^2
C_2H_2	18.52123	6.4074×10^{-6}	21.071	0.72047	0.99967
CO_2	21.15993	1.86027×10^{-7}	23.666	1	0.99988
CH_4	9.42552	1.20995×10^{-6}	16.750	1	0.99998

Table S6 Summary of pore textural and gas adsorption properties of **NOTT-101**, **ZJNU-35**, **ZJNU-18**, **ZJNU-19** and **ZJNU-20**.

MOFs		**NOTT-101**	**ZJNU-35**	**ZJNU-18**	**ZJNU-19**	**ZJNU-20**
$S_{BET}/S_{Langmuir}$ (m^2 g^{-1})		2755/2961	2591/2827	2391/2654	2165/2459	2154/2516
V_p (cm^3 g^{-1})		1.058	1.006	0.955	0.882	0.902
D_c (g cm^{-3})		0.6838	0.7001	0.7087	0.7284	0.7303
C_2H_2 uptake[a] (cm^3 g^{-1}, STP)	298 K	176.6	179.8	180.5	204.9	199.1
	295 K	186.8	189.1	191.5	214.5	210.0
	288 K	212.3	216.5	216.9	233.7	229.9
	278 K	258.1	258.3	254.9	262.4	258.2
CO_2 uptake[a] (cm^3 g^{-1}, STP)	298 K	85.0	88.4	88.4	106.5	103.8
	295 K	90.0	94.8	95.5	114.7	111.9
	288 K	109.1	113.8	115.0	136.9	133.1
	278 K	141.2	146.8	150.0	174.6	170.6
CH_4 uptake[a] (cm^3 g^{-1}, STP)	298 K	20.8	20.3	20.0	21.1	21.2
	295 K	21.2	21.5	21.3	22.5	22.6
	288 K	23.7	25.1	24.7	26.1	26.2
	278 K	29.0	30.9	29.9	32.5	32.4
C_2H_2/CH_4 (v/v = 1/1) IAST selectivity[a]	298 K	26.7	28.7	27.7	42.2	42.1
	288 K	30.3	31.8	32.1	50.6	50.9
	278 K	35.3	36.4	38.6	62.7	64.8
CO_2/CH_4 (v/v = 1/1) IAST selectivity[a]	298 K	4.8	5.2	5.1	6.4	6.2
	288 K	5.6	5.7	5.8	7.3	7.1
	278 K	6.6	6.5	6.7	8.5	8.3

$S_{BET}/S_{Langmuir}$ = BET and Langmuir surface areas; V_p = total pore volume; D_c = calculated framework density; [a] at 1 atm; STP = standard temperature and pressure